From Z-Machines to ALMA: (Sub)millimeter Spectroscopy of Galaxies
ASP Conference Series, Vol. TBD, 2006
A. J. Baker, J. Glenn, A. I. Harris, J. G. Mangum, and M. S. Yun, eds.

An Ultra-Wideband Receiver and Spectrometer for 74–110 GHz

Neal Erickson, Gopal Narayanan, Robert Goeller, Ron Grosslein

Department of Astronomy, University of Massachusetts, Amherst, MA 01002, USA

Abstract. A receiver system which covers the widest instantaneous bandwidth ever utilized by an astronomical heterodyne receiver is nearly complete. The entire 74–110.5 GHz band will be covered with a low noise frontend and a backend spectrometer having 31 MHz resolution. The receiver is intended for astronomical use in searching for the highly red-shifted spectral lines from galaxies of unknown redshift. The receiver uses InP MMIC based low noise amplifiers operated at 20 K, and operates with dual polarization feeds. The two receivers used with each feed are combined using a full band orthomode transition. Two such feeds are used in conjunction with a beam switch to maintain one dual polarized beam on the source at all times. The backend spectrometer is an analog auto-correlator built using very low cost microwave and analog/digital components.

1. Introduction

The advent of large format focal plane arrays of submillimeter and millimeter bolometer detectors such as SCUBA on the JCMT, BoloCAM on the CSO, MAMBO on the IRAM 30 m, and AzTEC on the JCMT has opened the window on distant star-forming galaxies. Ongoing continuum surveys have established the presence of a large population of dusty galaxies with relatively high rates of star formation (see review by A. Blain in this volume). The determination of the redshift distribution of this population of galaxies, referred to as SMGs (submillimeter galaxies), is an important task that is only now starting to gain pace with the construction of a new generation of instruments specifically targeted at this enterprise.

An ultra-wideband redshift search receiver and spectrometer is being built for this purpose at UMass. The receiver described here is intended for use on the Large Millimeter Telescope, a 50 m telescope now being built in Mexico, but it may find early use on the Haystack 37 m telescope, as well as a debugging period on the FCRAO 14 m telescope. Figure 1 shows the 5σ sensitivity limits for this receiver at different rotational J transitions of CO on these telescopes. On the same plot, the detections and upper limits of known SMG's from the survey of Greve et al. (2005) are also plotted. The assumptions that went into making the plot are listed in the figure caption. It is noteworthy that the average integration time for each of the detections in Greve et al. (2005) is ~ 11 hours, even though the approximate redshift was already known from optical observations. The Redshift Search Receiver on the LMT will detect most of the SMGs in Greve et al. (2005) in under 1 hour of integration. The Redshift Search Receiver on

the LMT will lead to the redshift identification of hundreds of other SMGs with unknown redshifts.

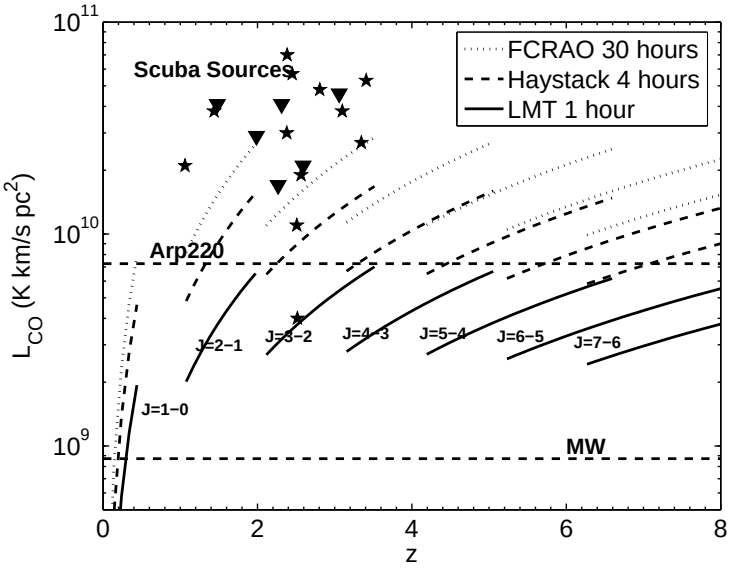

Figure 1. A plot of 5σ detection sensitivities for different J CO transitions with the Redshift Search Receiver on the LMT 50 m, the Haystack 37 m and FCRAO 14 m telescopes. Each segment represents a different CO rotational transition. The integration time for each telescope is marked in the plot. The assumed T_{SYS} are 80, 150K and 120K respectively for the LMT, Haystack and FCRAO telescopes. The respective antenna aperture efficiencies and space frame blockages are used in the calculation. The stars show the detected SMGs from Greve et al. (2005) and the triangles show the upper-limits for their non-detections. The detection sensitivities required to detect Arp 220 type objects at all redshifts are also marked on the plot.

2. Frequency Coverage

The ideal Redshift Search Receiver would be capable of measuring the redshift with a single observation. Given the fact that any of the lines in the CO ladder can appear at a particular frequency, the measurement of a single line is not sufficient to determine the redshift of an object and at least two lines must be observed to make this estimate unambiguously. Since the frequency spacing of the lines at a particular redshift, z, is

$$\Delta\nu = 115.3/(z+1) \ \ \mathrm{GHz}, \tag{1}$$

we can be assured of at least one line in the band for redshifts > 2 as long as the bandwidth of the spectrometer is greater than 38.4 GHz. However, to assure two lines in a randomly placed band requires 50% larger bandwidth, corresponding to $\sim$ 58 GHz. The latter number exceeds the entire width of the 3mm atmospheric window. In Figure 2, plots of the expected system temperature (T_{SYS}) of the Redshift Search Receiver in the 3mm band on the LMT is

shown. To show the effect of the atmosphere on T_{SYS}, two different levels of precipitable water vapor (PWV of 2mm and 5mm respectively) are shown. It can be seen that the atmospheric window restricts us to a choice of the band between $\sim$ 75 and $\sim$ 111 GHz (36 GHz bandwidth) for a low and reasonably flat value of Tsys. For reasons related to the performance of components in the receiver, this band has been modified to be 74–110.5 GHz.

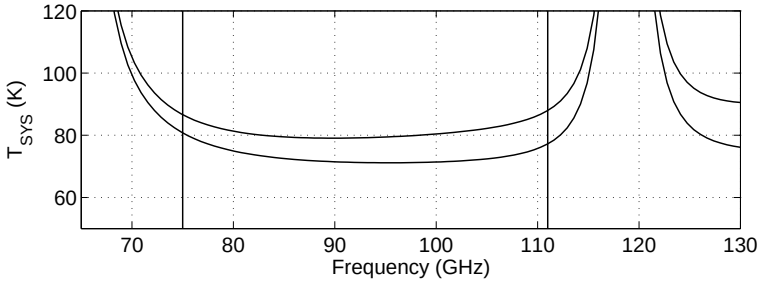

Figure 2. Expected on-the-sky noise temperature for conditions of 2 and 5 mm of precipitable water vapor, and a 60 K receiver noise temperature.

A more practical goal is to attempt to assure that at least one CO line is observable for any high redshift object and then use other information to resolve the ambiguity. In Figure 3, we show the redshift coverage for the Redshift Search Receiver. It should be noted that a receiver in the 3 mm window with 36.5 GHz bandwidth does an excellent job of covering the redshift space, with only a small gap for z $<$ 2 and another in the vicinity of z$\sim$ 2. Radio/FIR spectral indices (Carilli and Yun, 1999) suggest a median redshift of z$\sim$ 3 at 1 mJy. So, the gap in the lower redshift range of z$\leq$ 1.1 may not be very important. Compared to the overall redshift coverage of Redshift Search Receiver, the redshift gap around z=2 is small. And secondary indicators like CI, HCO^+ and HCN might be able to constrain the redshift even when two CO lines do not fall in the observing band at a lower redshift (see paper by Y. Min in this volume).

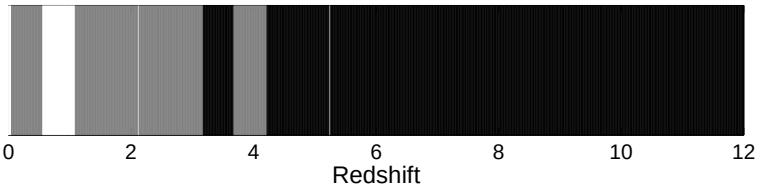

Figure 3. Redshift coverage for 74–110.5 GHz bandwidth. White has no CO line coverage, grey one CO line in band, and black two or more lines. CI provides a second line in the gaps for Z$>$ 3.

Given a detection of just one line or even a non-detection of any CO lines, there are a couple of ways to constrain the redshift. The submillimeter colors of the continuum emission can provide sufficient information in high redshift objects to make a crude estimate of the redshift and identify any line that is detected. Secondly, targeted follow-up measurements with receivers at other frequencies will be able to search for CO lines in the redshift range missed by

this receiver. Follow-up observations at another frequency such as in the 1mm band can also confirm the redshift derived from the Redshift Search Receiver and photometric analysis.

3. Frequency Resolution

The optimum sensitivity of a spectrometer is achieved when the resolution matches the width of the signal. The lowest cost of a spectrometer is usually achieved when the number of channels is kept to a minimum. Clearly, in a special purpose receiver it is important to select a resolution that will resolve the expected lines, but not by an excessive amount. Therefore, we have selected ~ 90 km/s as the resolution of the baseline instrument, since a channel of this width would resolve all the known high redshift objects. It is worth considering whether the choice of 90 km/s will make a substantial difference to the experimental results. For a given molecular mass, which predicts a particular integrated line intensity, the average flux density and detectability of the line increases as the line width is narrowed. Thus, molecular lines are most detectable when the kinematics of the underlying galaxy do not broaden them greatly. A natural limit is reached when the mass of the galaxy is dominated by molecular gas and the line width is directly related to the molecular mass. This is a situation that is far from true in normal galaxies, but in high redshift objects, the molecular gas masses appear to be an appreciable fraction of the total dynamical mass estimate. Thus, the velocity resolution sets a mass limit below which the object's emission will be diluted by the filter and the detectability of the line will fall with the square-root of the mass. For 90 km/s, this corresponds to a mass of a few $\times 10^9$ $M_\odot$.

4. System design

The Redshift Search Receiver is being built using several new technologies. A primary technological boost is given by the development of very low noise wideband MMIC amplifiers. These amplifiers use InP HEMT technology and have achieved noise temperatures as low as 30 K near 100 GHz (Weinreb et al. 1999). More typical amplifiers have noise below 50 K over much of the 74-111 GHz band. With the cascade of two of these devices a gain of 50 dB is available, and the noise properties of subsequent stages are relatively unimportant.

A second important development is in input waveguide components. For greatest sensitivity dual polarization receivers should be used with a single feed horn, and a very low loss waveguide polarization combiner has been developed which covers the full band. An additional critical development is a very fast electrical beamswitch using Faraday rotation in a ferrite.

Finally the backend of the receiver uses a very wideband analog autocorrelator built using microwave delay lines. This correlator has a useful bandwidth of 6.5 GHz in a single section, with 31 MHz resolution, and is built using very low cost components which have been developed for consumer audio and wireless applications.

The overall receiver design is similar to the 32 element SEQUOIA array (Erickson et al. 1999), with two stages of 20 K preamplification followed by

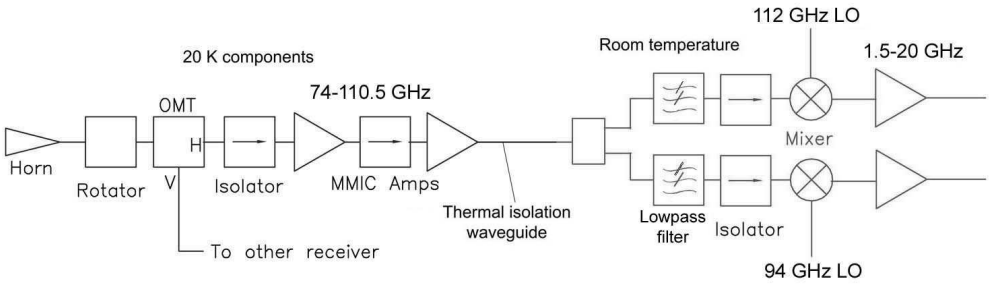

Figure 4. Block diagram of the receiver front end, showing 20 K and room temperature components separated by a waveguide section. Both mixers are operated at the same time.

downconversion to a very wide IF band. The block diagram is shown in Figure 4. The receiver is operated in dual polarization, and includes an electrical beamswitch on the input. Room temperature SSB mixers convert the entire band to two parallel IF channels.

The MMIC first stage amplifiers used in the receiver are the same as those used in SEQUOIA, except that they use an improved input network to flatten the gain and noise. These amplifiers use InP substrates and were designed at UMass and fabricated at TRW. These amplifiers have gain > 20 dB from 75–111 GHz. Two cold amplifiers are packaged in individual housings and are cascaded with interstage isolators, since it is not practical to directly connect the chips due to poor input and output match. Using a second stage amplifier of a different design, a gain of ~ 45–50 dB is maintained across the full band without increasing the gain ripple. The noise of all four amplifier pairs is shown in Figure 5, referenced to the waveguide flange of the input isolator.

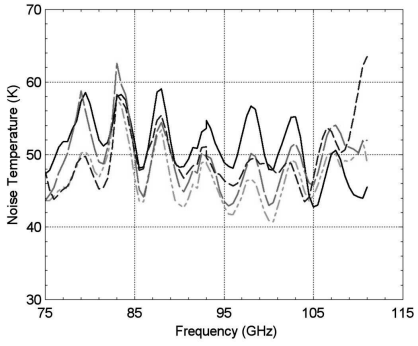

Figure 5. Noise temperature and gain of all four amplifiers, referenced to the input isolator waveguide flange.

For simplicity of operation, after these two 20 K gain stages, the signal passes through a thermal isolation waveguide to room temperature components. There the signal is split two ways and is down-converted by two mixers with

independent local oscillators (LO), each with an IF band of 1.5–20 GHz. By placing the LO's at 94 and 112 GHz, the IF bands meet in the band center, and complete coverage of the 36.5 GHz wide band is possible. Since mixer noise is unimportant, the mixers will actually be second harmonic mixers, and operate with LO's at 47 and 56 GHz. With these two LO's, there will be just one spurious signal in band at 94 GHz, and the nature of a second harmonic mixer makes this inherently weak, since only odd harmonics are radiated from the input. Because of the high gain ahead of the mixers, spurious signals do not have the potential to saturate following stages.

5. Input Network

The receiver will have two dual polarized beams with a beamswitch which interchanges the beams so that one beam remains on the source at all times. Dual polarized beams could be created using wire grid polarizers but these polarizers add considerable size to the system because they require an inconvenient configuration of the feeds, and they tend to add room temperature noise. Combining the receivers in waveguide into a wideband dual polarized feed is done using a new ortho-mode transition design with full band operation (Narayanan and Erickson 2002). The OMT has insertion loss below 0.3 dB across the WR10 band and a return loss > 18 dB. It uses a rather complex design but one which is straightforward to fabricate using CNC machining.

The MMIC amplifiers have significant 1/f gain fluctuations (Weinreb 1997) requiring a fast chop (~ 1 kHz) in order to get the best performance. Mechanical chopping is far too slow to fully overcome this noise. The fluctuations primarily affect their overall gain and make then unsuitable for continuum observations, but to a limited extent the gain noise also has a spectral character. While tests have shown that the spectral shape of this noise is fairly flat, varying on a scale of a few GHz, a fast chop will improve the data and permit the observation of very wide lines. Fast chops require electrical switches but prior to this no such switch had been built for the full WR10 band, and this system has an additional requirement of dual polarization. We have constructed an input beamswitch using a polarization rotator in the dual polarized input waveguide. This rotator in conjunction with an external polarizer makes a beamswitch as shown in Figure 6. With the polarization in one state, a beam passes through the grid, while at 90° rotation it is reflected. After an additional reflection (which is not shown) the beams will be parallel to each other, and a separation of ~ 3 HPBW may be achieved.

Such a switch is conceptually easy to implement using a polarization rotator based on Faraday rotation in a ferrite material. Ferrites are dielectrics having high magnetic permeability, so that significant Faraday rotation can occur in a very short length, and this rotation shows no frequency dependence. If a dual polarized beam is coupled into a ferrite with a switched magnetic bias, then both modes are rotated by the same amount. The problem in implementing this is in efficiently coupling the modes into a ferrite which can also easily have switched bias. The design works as follows. Tapered transitions at either end couple from square waveguide to waveguide of reduced cross section which gradually becomes filled with a dielectric rod. At the end of the transition the field is completely

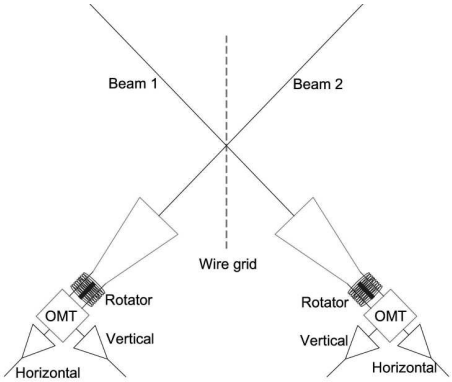

Figure 6. Layout of the input beams to the receiver showing the rotator beamswitch and OMT.

contained within dielectric and this dielectric then transitions to a ferrite rod. This assembly is small enough to be readily biased with an electromagnet. At the other end of the rod the field is reconverted to square waveguide. A cross section of the rotator is shown in Figure 7. The switching time of the rotator is $< 10\mu$s, allowing switching rates > 10 kHz. At this speed the receiver should have excellent continuum sensitivity.

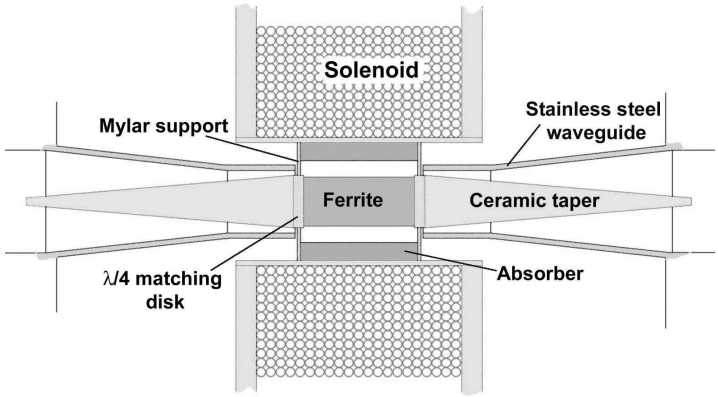

Figure 7. Cross section through ferrite polarization rotator. Input and output waveguides have square cross sections, while the ceramic tapers and the ferrite are circular.

6. Overall Performance

The complete system noise temperature of one pixel outside the dewar window with the polarizer biased to 45° rotation is shown in Figure 8. There is a lot of structure mostly due to the loss of the rotator but also due to the other input components. The other 3 pixels have similar average noise but somewhat higher noise at the peaks. There is a differential loss of $\sim 2\%$ between the + and −

rotation states which adds a frequency dependent receiver offset, but if the sky and the rotator are at the same temperature this offset disappears. The rotator is at 18–20 K and under good weather the sky should be within 10–20 K of this temperature so the offset is < 0.4K. Beam switching by exchanging the on and off source beams periodically should remove this offset.

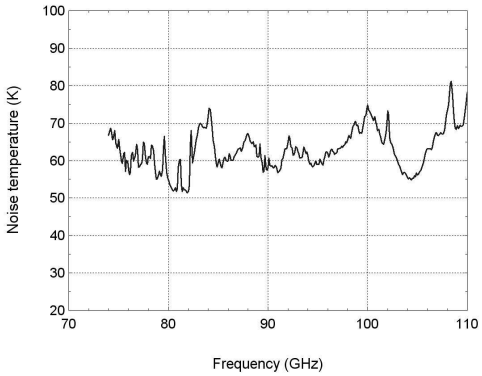

Figure 8. Complete receiver noise temperature of one pixel of the receiver including all input losses.

7. Backend AutoCorrelator

The four receivers making up this system have a combined IF bandwidth of 146 GHz, and the entire band needs to be spectrally processed simultaneously. With a resolution of 30 MHz, ~ 5000 spectral channels are needed. A technique using analog autocorrelation (Harris and Zmuidzinas 2001) seems most suitable, and in this work the method has been refined to cover much wider bandwidth in a single spectrometer at significantly lower cost. The basic technique is shown in Figure 9, in which a wide band signal is split two ways and sent in opposite directions down a delay line. Taps on the line sample a small amount of the signals from both directions, and the tapped signals from opposite directions are then multiplied. The set of multiplied tapped signals forms the autocorrelation function, which can then be Fourier transformed to generate the spectrum.

In this design, the delay lines cover a frequency range of 0–8 GHz. Actual multipliers are not needed, but instead the tap signals are simply summed and detected with biased silicon diodes. A square law detector is an excellent multiplier in this application, but it also produces total power terms. If the two signals arriving at a tap are A and B, the detector output is:

$$A^2 + B^2 + 2AB \tag{2}$$

and the only part that is desired is AB. The unwanted parts are readily eliminated by phase switching the signal to one delay line by 180°, which causes the sign of only the AB term to change. AC processing of the signal captures only the desired part. A wideband 0–180° phase switch based on a balanced mixer is a standard component, and these show excellent amplitude balance. Biased

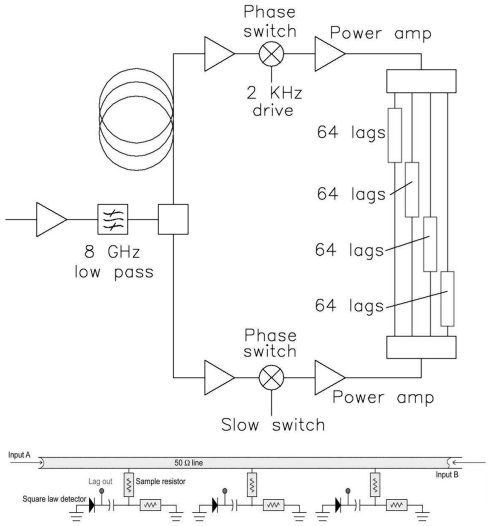

Figure 9. Schematic diagram of the analog autocorrelator. The top is an overall view while the bottom is a detail of just the tapped delay line. The tap resistors are 1500 Ω to weakly sample the signal.

silicon diodes make excellent square law detectors, with a very wide dynamic range, and these diodes are also very inexpensive.

The principal drawback to the use of detectors rather than multipliers is their sensitivity to the total power signal as well as the multiplied cross-term. While phase switching removes the time average, it cannot remove the noise since this is also AC. Any total power fluctuations should be entirely a common mode signal to all detectors, and so there should be no net response after compensation for the different gains, but any variation in detector frequency response creates individual signals. In the worst case this noise can be very large, so the detectors must be well matched.

Practical considerations reduce the useful bandwidth of the correlator. One problem is that all of the tap mismatches add up to cause a significant VSWR below 0.5 GHz, so this part of the band is not usable. In addition, multi-octave components working up to 8 GHz are rare, particularly phase switches and power splitters, and the maximum bandwidth for low cost parts is 1.5–8 GHz. Since the bandwidth is so large, there is no serious penalty in throwing away some bandwidth, and in this case it actually reduces the overall cost.

The delay lines and the A/D converters are all assembled into a single six-layer, double sided circuit board, with 64 lags in each subunit (one tapped line) and 256 lags on a complete circuit board. The larger delays are implemented with external lines using coaxial cable. The delay line layer of the board is on $\epsilon = 2.33$ material with a tap spacing of 6 mm, which is about as close as is practical with standard (0402 size) components and assembly practices. This makes a 64 lag subunit 39 cm long (in a U-bent line), and the detector amplifiers and A/D converters all fit tightly within this length. With a maximum frequency

of 8 GHz, the resolution of a board is 31 MHz, and each board covers 6.5 GHz, so 24 boards are needed to cover 146 GHz with 0.5 GHz overlaps between boards.

The AC signal (at 4 kHz) from each detector diode is amplified and digitized using an 18 bit $\Sigma\Delta$ audio A/D converter with 48 kHz sample rate. An FPGA on each board multiplexes the A/D converter outputs, and all subsequent signal processing is digital within the FPGA. This includes digital synchronous detection with three chops within system; phase switches at 2 kHz and 4 kHz, and the 1 kHz input beam switch. A total power switch is used to calibrate the response of the detectors to the system noise. Each board is 23$\times$ 32 cm and six boards and their drivers fit within a VME chassis along with a VxWorks OS PowerPC computer. Short integrations are performed within the FPGA, with long accumulations in the PowerPC through interrupt service routines

Two driver amplifiers are used for each set of 256 taps, with their output passively split into each subgroup of 64 taps. This eliminates problems that might occur with independent amplifiers driving sets of 64 lags. Each set of 64 lags requires 5 mW of drive (on each line) to sufficiently overcome detector noise, and there are 4 such lines, requiring about 25 mW drive to the 4 way splitter. The driver amplifier module includes the coaxial delay lines.

So far tests are being performed on just a prototype board having a number of fabrication errors, so results may not be entirely typical of production. The spectrometer is calibrated using a set of monochromatic frequency inputs covering the full band, and a basis set of functions is derived which are approximately cosines (Harris and Zmuidzinas 2001). These are used to derive the spectrum from the autocorrelation function. A simple cosine transform works fairly well but some spurious features are observed in the spectrum. Detector gains are calibrated relative to each other and any offset in the autocorrelation function due to total power fluctuations is removed before transforming. Long integrations have been made to determine the spectrometer stability and noise level. With a simulated slow beamswitch, the Allan variance time is > 40 sec, with the spectrometer having no temperature stabilization. The spectral noise is elevated over the radiometric expectation by 19-20% with an 8 GHz bandwidth signal input, for reasons that so far have not been determined. With a relatively narrow band input of 700 MHz, the noise is at exactly the radiometric value within the signal band but outside the band there is much more noise than just the spectrometer internal noise. There appears to be some mechanism to spread noise across the full band due to errors in the transform that are not properly compensated. There are several ways this can happen, the most likely, as mentioned previously, through detectors that have variations in frequency response. Almost all detectors have the same response to within 1–2 dB, but some are quite different due to PC board over-etching and bad component placement. Work is continuing to investigate this problem, but it is not so serious, since digital correlators routinely accept a similar penalty.

The prototype spectrometer has been tested as a backend to the SEQUOIA receiver system, and Figure 10 shows a spectrum of 6 GHz of bandwidth taken in 100 minutes of integration on the first night of tests, looking toward M82. This spectrum was taken in conventional position switched mode, 15sec on source and 15sec off, and shows the potential to obtain the very flat baselines needed.

The Redshift Search Receiver will include the fast beamswitch, which should make the baselines even better. These tests will begin in April 06.

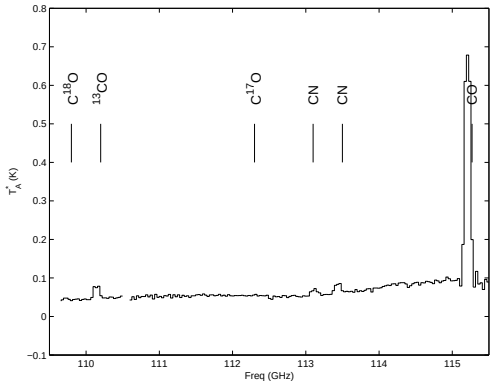

Figure 10. Spectrum of M82 taken in 100 minutes of integration with SEQUOIA and the autocorrelation spectrometer at the FCRAO 14 m telescope. No velocity correction is applied, so the lines are slightly offset from the rest frequencies noted. No baseline is removed, showing the flatness that is inherent to the system. The general baseline shape is due to the large variation in atmospheric background across the band. A spurious receiver line due to LO reference leakage has been removed near 110.5 GHz.

8. Conclusions

A receiver system is being built having very low noise over the full WR10 band, including new full band waveguide components for polarization combining and beamswitching. The IF signal is spectrally processed with a backend spectrometer consisting of an analog autocorrelator having a total bandwidth of 146 GHz with a resolution of 31 MHz. The spectrometer is very low in cost compared to other alternatives. The receiver is expected to deliver flat spectral baselines over the entire frequency range through the use of a fast input switch.

Acknowledgments. This work was supported by the National Science Foundation under grant AST-0096854.

References

Erickson, N. R., Grosslein, R. M., Erickson, R., and Weinreb, S., 1999, IEEE Trans. Microwave Theory and Tech., pp.2212-2219, Dec 99.

Greve, T. R., et al. 2005, MNRAS, 359, 1165

Harris, A. I., and Zmuidzinas, J., 2001, Review of Scientific Instruments, pp 1531-1538, Feb 01.

Narayanan, G., and Erickson, N. R., 2002, Thirteenth International Symposium on Space Terahertz Technology, pp. 505-514, Apr. 02.

Weinreb, S., Lai, R., Erickson, N. R., Gaier, T., and Wielgus, J., 1999, Proceedings of 1999 IEEE MTT-S International Microwave Symposium, Anaheim, CA, June 99.

Weinreb, S., North American URSI Meeting, Montreal, P.Q., Canada, July 1997, pg 644.